Multidimensional NMR Studies of Poly(ethylene-*co*-1-butene) Microstructures

Sangrama K. Sahoo, Tong Zhang, D. Venkat Reddy, and Peter L. Rinaldi*

Department of Chemistry, The University of Akron, Akron, Ohio 44325-3601

Lester H. McIntosh and Roderick P. Quirk

Department of Polymer Science, The University of Akron, Akron, Ohio 44325-3909

Received January 23, 2003

ABSTRACT: The microstructures, including tacticity (triad and tetrad stereoconformation) and comonomer sequence distribution, of poly(ethylene-*co*-1-butene) copolymer with different 1-butene contents were investigated by high-temperature (120 °C) two-dimensional (2D) nuclear magnetic resonance (NMR) spectroscopy at 750 MHz. The microstructures of these copolymers were analyzed by the combination of different NMR techniques including quantitative ^{13}C NMR, ^{13}C DEPT (distortionless enhancement by polarization transfer), pulsed-field-gradient (PFG) $^{1}H-^{13}C$ heteronuclear single quantum coherence (gHSQC), and heteronuclear multiple bond coherence (gHMBC). High temperature, along with multidimensional PFG NMR, facilitates the study of poly(ethylene-*co*-1-butene) copolymers by improving the resolution of resonances which otherwise have short T_2 (spin−spin) relaxation at ambient temperature. The combined information from 2D $^{1}H-^{13}C$ gHSQC, gHMBC, and quantitative ^{13}C NMR experiments provided unambiguous resonance assignments from triad, tetrad, and, in a few cases, pentad comonomer sequence distributions of poly(ethylene-*co*-1-butene) with improved resolution in the regions of the spectrum containing the resonances of structures associated with ethyl branches. The copolymer with 41% 1-butene content synthesized using the metallocene catalyst system [$(C_5Me_4)SiMe_2N(t\text{-}Bu)$]$TiMe_2$/MAO shows a mixture of both meso and racemic diads with predominantly racemic configuration, while another commercially available copolymer with 12% 1-butene content shows predominantly meso diads. Quantitative analysis of comonomer sequence distributions was determined from ^{13}C NMR data analysis.

Introduction

Ever since the commercialization of copolymers of ethylene and α-olefins in 1968 by the Phillips Petroleum Co.,[1] much attention has been devoted to this area of research. In 1980s, the development of group IV metallocene homogeneous catalysts and methylaluminoxane (MAO) cocatalyst systems[2] yielded polymers having narrow molecular weight distributions along with stereo- and regioregular polymers with specific comonomer sequence distributions.[3,4] Linear low-density polyethylenes (LLDPE) were produced commercially by copolymerization of ethylene and α-olefins, such as 1-butene, 1-hexene, and 1-octene, using these catalyst systems. To understand the mechanism of polymerization, it is necessary to gather information on the comonomer sequence distribution, which provides information on propagation step, as well as the structure of the end groups, which give information on the initiation and termination steps. Also, a detailed knowledge of microstructure including the stereosequence distribution in these copolymers would be useful in the optimization and development of new generations of metallocene catalysts for synthesizing copolymers with well-defined microstructures. Our first attempt in this direction resulted in the unequivocal assignments of hexyl chain branches as well as chain ends in poly(ethylene-*co*-1-octene) copolymers by a high-temperature multidimensional NMR approach.[5] It was possible to detect different resonances from microstructures which are present at low occurrence levels, minimizing the error in the quantitative analysis of comonomer composition.

Tacticity and degree of stereoregularity are important aspects of polymer microstructure that affect polymer properties such as optical clarity, strength, stiffness, and melting point. For example, syndiotactic polypropylene has a lower crystallinity than isotactic polypropylene.[6] Although 1D ^{1}H and ^{13}C NMR are considered the most useful methods for quantifying a polymer's stereochemical purity,[7−11] modern multidimensional NMR techniques provide better means for establishing stereosequence assignments.[12,13] For example, Cheng et al.[14,15] have used 2D $^{13}C-^{1}H$ heteronuclear shift-correlated (CSCM)[16] and homonuclear shift correlation (COSY) experiments[17] to characterize isotactic and atactic polypropylene. Li and Rinaldi[18] used a three-dimensional (3D) $^{1}H/^{13}C/^{19}F$ triple-resonance NMR experiment to determine the tacticity in the triad stereosequence arrangement of poly(1-chloro-1-fluoroethylene).

With the development of modern computers, new generations of high-field and high-sensitivity NMR spectrometers, and 2D and 3D NMR techniques which disperse resonance information into a second or third frequency dimension,[19−21] NMR has become an increasingly useful method to obtain information about polymer structures. However, only a few papers on 2D and 3D NMR of polyethylene and polyethylene-based copolymers have been published.[12,14,18,22−24] The paucity of experimental work is partially attributed to difficulty in performing these experiments. The poor mobility of polymers lead to rapid T_2 relaxation, greatly reducing signal intensity in 2D NMR experiments, such as HMBC[25] experiments, that are based on coherence

* Corresponding author. Telephone: 330-972-5990. Fax: 330-972-5256. E-mail: PeterRinaldi@uakron.edu.

10.1021/ma030056o CCC: $25.00
Published on Web 05/03/2003

transfer via small long-range J couplings. To solve this problem, high-temperature NMR is required to increase the molecular mobility and hence to narrow the spectral lines (e.g., polyethylene-based copolymers are typically analyzed at 120 °C). On the other hand, pulsed field gradient (PFG)[26] techniques that take the place of the traditional phase cycling methods for coherence selection of the weak signals from ^{1}H bound to ^{13}C, while suppressing the large signals from ^{1}H bound to ^{12}C. This method not only saves time but also drastically reduces the t_1 noise by optimizing the use of the spectrometer dynamic range. Until recently the design of NMR probes for PFG methods precluded their use at the high temperatures used for many polymer NMR studies. The recent availability of PFG probes for high temperature NMR permits the detection of the weak 2D-NMR signals needed to assign the resonance from low occurrence polymer structures. In this work gHSQC was used rather than PFG−heteronuclear multiple quantum coherence (gHMQC) NMR as it provides better resolution of the cross-peaks from the tightly coupled spin systems of ethylene-α-olefin copolymer. These systems resemble the spin systems of peptides and proteins, where it is well documented that HSQC gives better resolution in ^{1}H−^{15}N correlation spectroscopy.

To explore the microstructure of ethylene-α-olefin copolymer by the multidimensional NMR methods, we chose a commercially interesting and widely studied copolymer, poly(ethylene-*co*-1-butene). Poly(ethylene-*co*-1-butene) copolymers were extensively characterized by NMR,[27−34,35] differential scanning calorimetry (DSC),[36,37] wide-angle X-ray diffraction (WAXD),[38] size exclusion chromatography (SEC),[39] and infrared spectroscopy (IR)[40] for the determination of microstructure with varying synthesis conditions. The statement by Randall[31] in 1989, that the assignments for ethylene-1-butene copolymer were only partially complete and the effects of chirality and inversion are not established, is still true. Previous assignments of NMR resonances to specific comonomer sequences were made by comparing the resonance integral intensities with the statistical probabilities of forming each possible sequence and by comparing observed chemical shifts with those of model compounds or reference polymers.[30−32,34] However, use of these methods of assignment often leads to misleading information as the chemical environments, and thus observed chemical shifts in the actual polymer are influenced by long-range interactions as well as the stereochemical configurations at various branching sites. As shown recently by Busico et al.[41] in the case of ethylene/propylene copolymer, although high field ^{13}C NMR can give good insight into a polymer's regio- and stereo-sequence distribution, a full unambiguous assignment is not possible without complementary 2D NMR data. Thus, in this work, the tacticity and comonomer sequence distribution of two poly(ethylene-*co*-1-butene) copolymers with different 1-butene content have been investigated using high-temperature gHSQC[42−45] and gHMBC[25] ^{1}H−^{13}C 2D and ^{13}C 1D, ^{13}C DEPT[46] techniques on a 750 MHz NMR spectrometer. Detailed comonomer sequence assignments were obtained by combining the results from 1D and 2D NMR data. The samples studied are copolymers of ethylene and 1-butene, one polymer synthesized using metallocene catalyst system [(C_5Me_4)$SiMe_2$N(*t*-Bu)]$TiMe_2$/MAO[47] contains about 41% 1-butene, and the other is a commercial copolymer having 12% 1-butene content. The [(C_5Me_4)-$SiMe_2$N(*t*-Bu)]$TiMe_2$/MAO catalyst system permits the production of copolymers with high α-olefin contents.[48] It has been found that polypropylene synthesized using this kind of catalyst system contains 72% syndiotactic triads, showing a moderate amount of syndiotacticity.[49] The different tacticities of these two poly(ethylene-*co*-1-butene) samples are demonstrated.

Experimental Section

Preparation of Polymers. Two ethylene/1-butene copolymers with different percentages of 1-butene were used for the present studies. Copolymer A containing about 12 mol % 1-butene was purchased from Aldrich Chemical Co. and was used as received; copolymer B with about 41 mol % 1-butene was synthesized with a metallocene catalyst system [(C_5Me_4)-$SiMe_2$N(*t*-Bu)]$TiMe_2$/MAO.[49]

Preparation of Polymer Samples for NMR Analysis. All samples were dissolved in a 60% 1,4-dichlorobenzene-d_4/40% 1,2,4-trichlorobenzene (v/v) solvent mixture to produce ca. 7% (w/v) polymer solutions. To obtain homogeneous solutions, the samples were heated to 120 °C and rotated at 20 rpm in a Kugelrohr oven for 2 h, and then at 100 °C for 10 h more. A trace of hexamethyldisiloxane (HMDS) was added to the original solvent mixture to serve as an internal chemical shift reference both in 1D and 2D NMR spectrum (δ_H = 0.09 ppm, δ_C = 2.03 ppm).

1D Quantitative ^{13}C NMR. Quantitative ^{13}C NMR experiments were performed at 188.6 MHz using a 10 mm broadband probe (^{15}N−^{31}P) on a Varian UNITYplus 750 MHz spectrometer at 120 °C. The experimental parameters were set as follows: 12.5 μs π/2 pulse, 22.5 kHz spectral width, 1024 transients, 2.5 s acquisition time, and a 25 s relaxation delay for quantitative analyses. Spectra were obtained with full NOE and Waltz-16 decoupling. Data were zero filled to 256K and exponentially weighted with 0.5 Hz line-broadening before Fourier transformation. The ^{13}C DEPT experiments were performed under the same condition as quantitative ^{13}C NMR, but with a 3 s relaxation delay and a 20.5 μs π/2 ^{1}H decoupler pulse.

2D gHSQC NMR. Gradient-assisted 2D HSQC (gHSQC) spectra were collected on the same spectrometer with a Nalorac H/C/N 5 mm PFG probe operated at 120 °C. The π/2 pulse widths for ^{1}H and ^{13}C were 10.25 and 14.5 μs, respectively. Data were acquired using the following parameters: a relaxation delay of 1 s, a delay Δ set to 1/(2 × $^1J_{CH}$) ($^1J_{CH}$ = 125 Hz), for optimizing the intensities of cross-peaks from one bond ^{1}H−^{13}C correlations, and an acquisition time of 0.256 s with simultaneous ^{13}C GARP1 decoupling. A total of 24 transients were averaged for each of 2 × 1024 increments during t_1 for phase sensitive gHSQC based on the States method.[50] The evolution time was incremented to provide the equivalent of an 8.0 kHz spectral width in the f_1 dimension, and a 1.0 kHz spectral width was used in the f_2 dimension. At the beginning of each relaxation period, a ^{1}H 90° pulse sandwiched by two homospoil gradient pulses (having 0.175 T/m strength and 10.0 ms duration) were applied to destroy transverse magnetization. The third and fourth gradient pulses were 0.175 and 0.088 T/m, respectively, with 1.0 ms duration for the coherence selection between ^{13}C and ^{1}H. Linear prediction was used to forward extend the data two to four times its original length, to compensate for the short acquisition time as well as the relatively small number of points in the evolution time dimensions. Data were zero filled to provide a 2048 × 4096 matrix and processed with sinebell and shifted sinebell weighting before Fourier transformation.

2D gHMBC NMR. The π/2 pulse widths for ^{1}H and ^{13}C were 10.25 and 14.5 μs, respectively. Data were acquired using the following parameters: a relaxation delay of 1.0 s, a 1.0 s acquisition time, a delay Δ set to 1/(2 × $^1J_{CH}$) ($^1J_{CH}$ = 125 Hz) for suppressing the 1-bond ^{1}H−^{13}C correlations, and τ delays of 50.0 and 100.0 ms (set to 1/(2 × $^nJ_{CH}$) to get two separate spectra with delays optimized for two- and three-bond ^{1}H−^{13}C correlations. The strengths of two 2.0 ms gradient pulses

Scheme 1. Some Possible Monomer Sequences for Poly(ethylene-*co*-1-butene)

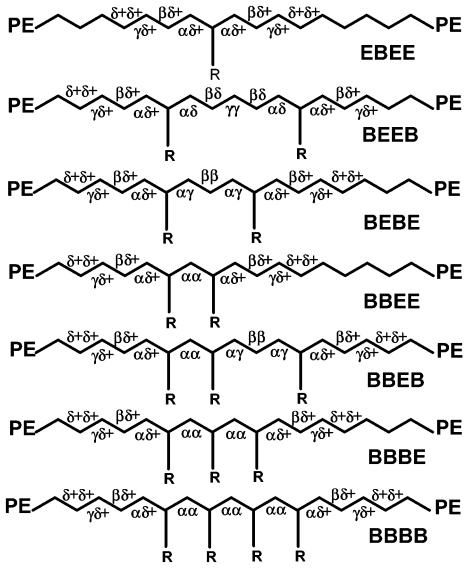

were 0.175 and 0.131 T/m, respectively (for the coherence selection between ^{1}H and ^{13}C). A total of 24 transients were averaged for each of 1024 t_1 increments. The evolution time was incremented to provide the equivalent of an 8.0 kHz spectral width in the f_1 dimension. A 1.0 kHz spectral width was used in the f_2 dimension. Linear prediction was carried out in the f_1 dimension to improve the resolution compensating for the limited number of t_1 increments. Data were zero filled to provide a 4096 × 8192 matrix and processed with sinebell and shifted sinebell weighting before Fourier transformation.

Results and Discussion

Nomenclature and Structure. The nomenclature used for assigning the carbons in poly(ethylene-*co*-1-butene) copolymer was first described by Carman[51] and later refined by Randall.[31] For polymer backbone carbons, a pair of Greek letters are used to represent a carbon atom distances to the branch points in either direction. Carbon atoms in the side-chain branches are identified by iB_n where "i" indicates the carbon position in the branch, with the methyl carbon in position "1", and the subscript "*n*" indicates an *n*-carbon branch. The saturated end group carbons in the main chain are designated by 1s, 2s, and 3s starting with methyl carbon at the chain end as position "1".

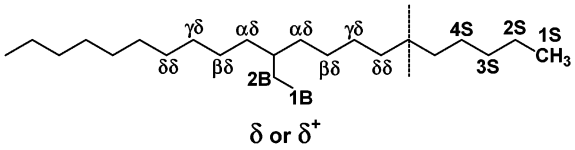

At high field, the chemical shifts of carbons in a particular monomer unit are sensitive to the structures of adjoining monomer units and, in some cases, to the structures two monomer units away. In these cases, the simple two-letter labeling of carbon atoms becomes insufficient, and the *n*-ad (triad or tetrad) sequence must also be specified. Scheme 1 shows possible tetrad sequences of poly(ethylene-*co*-1-butene) copolymers, where "E" and "B" indicate ethylene and 1-butene monomer units, respectively.

1D ^{13}C NMR Analysis. The extreme sensitivity of ^{13}C NMR chemical shifts to variations in microstructural environment of copolymer backbone is demonstrated by

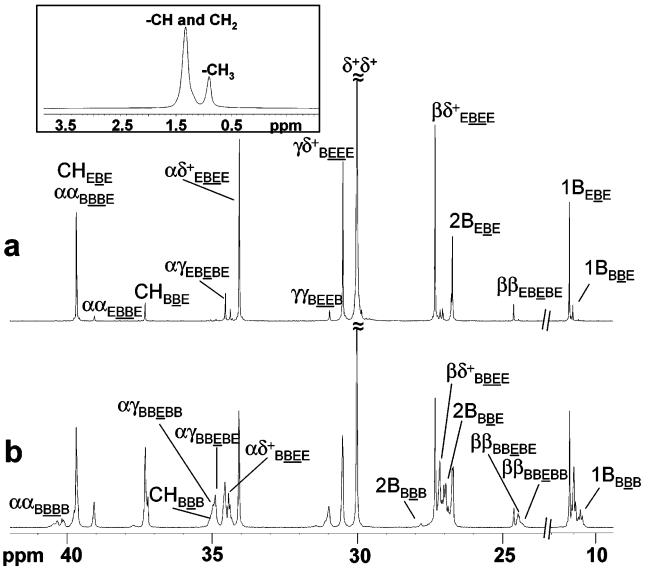

Figure 1. Aliphatic regions from the 188.6 MHz 1D ^{13}C NMR spectra of poly(ethylene-*co*-1-butene): (a) copolymer A, containing 12% 1-butene, and (b) copolymer B, containing 41% 1-butene. (Inset: 750 MHz ^{1}H NMR spectrum of copolymer B.)

comparing the spectra obtained at 120 °C of poly(ethylene-*co*-1-butene) copolymers with two different 1-butene contents (Figure 1). Introduction of 1-butene units as comonomer produces ethyl branches on the copolymer backbone and contiguous 1-butene sequences lead to 1,3-diethyl and 1,3,5-triethyl branches etc.[31] The ^{1}H NMR spectra of both the copolymers show only two resonances (insert in Figure 1 (^{1}H NMR spectrum of copolymer B)), a peak at 0.9 ppm corresponding to methyl ($-CH_3$) protons and a strong peak at 1.2 ppm corresponding to all the methylene ($-CH_2-$) and methine (>CH−) protons. The spectral feature indicates the strong overlap among the polymer backbone protons and thus an overall strongly coupled spin systems. Figure 1a shows the spectrum of copolymer A (ca. 12% 1-butene); Figure 1b shows the spectrum of copolymer B (ca. 41% 1-butene). It was shown in earlier studies of poly(ethylene-*co*-1-octene) that 120 °C is the most suitable temperature for producing spectra with optimal sensitivity and resolution from these samples.[5] The segmental mobility of polymer chains increases dramatically with the increase in temperature, resulting in the narrow resonance line widths and better resolution. This was evident particularly in detecting weak resonances buried under the tails of adjacent strong resonances. In the ^{13}C NMR spectra, CH and CH_2 carbons from both the main chain and ethyl branches are found in the 24.0−42.0 ppm range, while the resonances of CH_3 groups, corresponding to ethyl branches, appear at 10.0−12.0 ppm. The low intensity resonances at 14.0, 23.0, and 32.0 ppm from saturated chain ends are observed in copolymer A, however, these signals are not detected in the spectrum of copolymer B. The absence of these resonances in copolymer B shows that isolated saturated chain ends are too low in concentration to be detected by ^{13}C NMR. The ^{13}C NMR spectrum in Figure 1a is relatively simple when compared with the spectrum in Figure 1b, as the probability of forming comonomer sequences containing two or more 1-butene units increases dramatically at higher 1-butene content. (The probability of forming sequences with *n* consecutive B units is related to $f_B{}^n$, where f_B is the mole

fraction of B units in the reaction mixture.) The 188.6 MHz ^{13}C NMR spectrum of copolymer B (Figure 1b) shows many new features in terms of well-resolved resonances compared to previously reported low field data.[31,32,34] The better resolution and dispersion will permit identification of the degree of stereoregularity and provide evidence on the presence of higher *n*-ad sequences such as tetrad, pentad, hexad, etc. The resonances of methylene groups near two branch points appear at 39.0−42.0 ppm ($\alpha\alpha$ methylene resonances) and 24.0−25.0 ppm ($\beta\beta$ resonances). The methylene resonance from isolated $\gamma\gamma$ carbons is well-resolved at 30.9 ppm. The main chain resonances appear at the following chemical shifts: $\alpha\delta^+$ at 33.5−34.5 ppm; $\beta\delta^+$ at 26.5−28.0 ppm; $\gamma\delta^+$ at 30.5 ppm and $\delta^+\delta^+$at 30 ppm. In the 40.0−42.0 ppm region of the spectrum in Figure 1b, several $\alpha\alpha$ methylene resonances from long B sequences (e.g., $\alpha\alpha_{BBBB}$) can be clearly observed. However, only a single $\alpha\alpha$ methylene resonance at 39.21 ppm from sequences containing two consecutive B units ($\alpha\alpha_{EBBE}$) is observed in the spectrum of the polymer with the lower 1-butene content (Figure 1a). There is overlap of the $\alpha\alpha_{BBBE}$ and CH_{EBE} resonances at 39.76 ppm though it is not clear from 1D ^{13}C NMR spectrum (vide infra). Similarly, resonances such as those previously attributed to CH_{BBE} (37.45 ppm), CH_{BBB} (35.23 ppm), $\beta\beta_{EBEBE}$ (24.68 ppm), and $1B_{BBE}$ (11.02 ppm) are also considerably weaker in the spectrum in Figure 1a when compared with the spectrum in Figure 1b. In the methyl region (10−11.5 ppm), at least three resonances ($1B_{EBE}$, $1B_{BBE}$, $1B_{BBB}$) are resolved in Figure 1b, while only $1B_{EBE}$, $1B_{BBE}$ resonances are observed in Figure 1a. Interestingly, the upfield resonances at 10.6 and 10.9 ppm due to $1B_{BBB}$ and $1B_{BBE}$ carbons appear to be split into triplets with additional unresolved features. These triplet features could be attributed to either different triad stereosequences (*mm*, *mr*, and *rr*) and/or to higher pentad comonomer sequences. Although it is possible to explore the stereosequence and comonomer-sequence distributions, by using high field and high temperature, as seen in the spectrum in Figure 1b, it is still not sufficient to eliminate all the overlapping resonances and obtain unequivocal assignments from the 1D spectrum. These resonances can be distinctly resolved with the aid of 2D ^{1}H−^{13}C gHSQC NMR spectra (see below), in which chemical shift information is dispersed in two dimensions.

Most of the observed resonances in the ^{13}C NMR spectra are from methylene carbons; however, the DEPT experiment helps to identify the resonances from the few unique methine and methyl carbons. The results of a DEPT experiment are summarized in column 5 of Table 1, and the edited spectra of copolymer B are presented in the Supporting Information. The ^{13}C chemical shift assignments of resolved peaks are listed in Table 1 along with literature assignment.[30−34] Peak regions labeled A−G in the first column are based on the groups of peaks resolved by Hsieh and Randall.[30,31] These regions are further subdivided and labeled with numerical subscripts (e.g., region A is subdivided into regions A_n−A_m) as shown in the second column, based on resolved peaks in the 188.6 MHz ^{13}C NMR spectra.

A set of reliable chemical shift assignments is important for quantitative analysis. Data from the 2D ^{1}H−^{13}C gHSQC and gHMBC NMR experiments provide the means of unambiguously identifying structure fragments in the copolymer and of obtaining unequivocal resonance assignments.

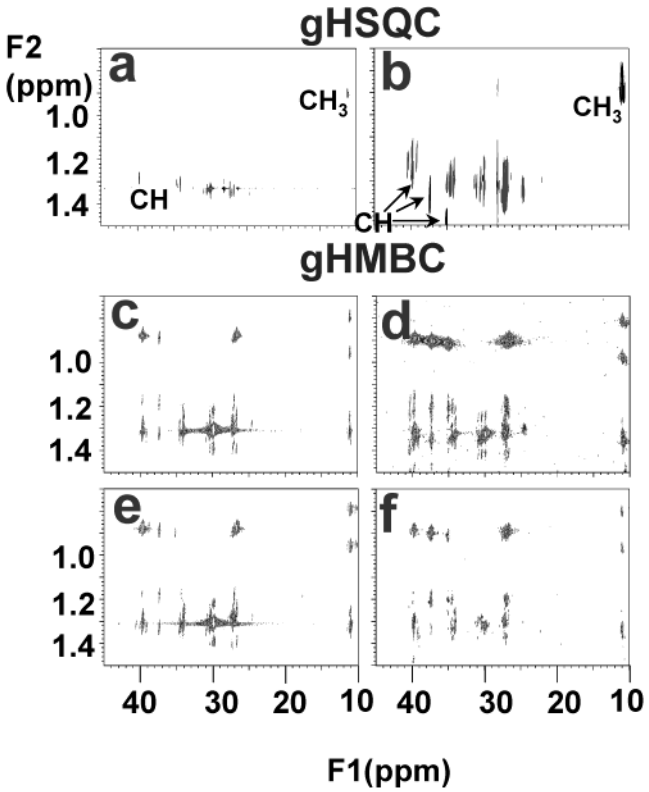

Figure 2. 2D ^{1}H−^{13}C gHSQC and gHMBC (with two different delays optimized for selective observation of two- and three-bond ^{1}H−^{13}C couplings (τ_{mb} = 0.05 and 0.1s)) spectra of copolymer A and B obtained at 750 MHz: (a) gHSQC spectrum of copolymer A; (b) gHSQC spectrum of copolymer B; (c) gHMBC spectrum (τ_{mb} = 0.05) of copolymer A; (d) gHMBC spectrum (τ_{mb} = 0.05) of copolymer B; (e) gHMBC spectrum (τ_{mb} = 0.1) of copolymer A; (f) gHMBC spectrum (τ_{mb} = 0.1) of copolymer B.

2D gHSQC and gHMBC of Poly(ethylene-*co*-1-butene). The 2D ^{1}H−^{13}C gHSQC experiment produces a spectrum with peaks correlating the chemical shifts of ^{1}H and directly bound ^{13}C atoms. The gHMBC experiment produces a spectrum with peaks correlating the chemical shifts of ^{1}H and ^{13}C atoms that are two and three bonds away. Combined data from gHSQC and gHMBC spectra provide unambiguous resonance assignments and detailed structure information. High-temperature NMR at 120 °C of these high melting and low solubility poly(ethylene-*co*-1-butene)s provides a means to increase the transverse relaxation times, resulting in narrow spectral lines that facilitate collection of high quality multidimensional NMR data. PFG coherence selection techniques also help in decreasing the experimental time and efficiently suppressing undesired signals and spectral artifact.[52] It has been established that PFG coherence selection and collection of spectra at high temperature are essential for achieving the dynamic range needed to detect multidimensional correlations from low occurrence structures such as polymer chain ends and branching structures.[19]

Parts a and b of Figure 2 show phase-sensitive gHSQC spectra of copolymers A and B respectively, showing one bond correlation between ^{1}H and directly bonded ^{13}C. Many cross-peaks are observed in the spectra due to different microstructures. The chemical shifts of these cross-peaks match well with the peaks

Table 1. Chemical Shift Assignments and Quantitative Analysis of Copolymers from Ethylene (E) and 1-Butene (B)

region		assignments		DEPT + HSQC[a]	δ^{13}C previous works			δ^{13}C[b] this work		δ^{1}H[c] this work		T_1 value[d]	integral value	
Randall	this work	carbon	polymer sequence	mult	Randall[7]	Cheng[13]	Rossi[9]	copolymer A E/B = 88:12	copolymer B E/B = 59:41	copolymer A E/B = 88:12	copolymer B E/B = 59:41	copolymer A E/B = 88:12	copolymer A E/B = 88:12	copolymer B E/B = 59:41
A	A_1	αα	B*BB*B	t					40.52		1.28, 1.33			
	A_2								40.45		1.23, 1.31			
	A_3								40.42		1.22, 1.30			
	A_4								40.34		1.26			
	A_5								40.29		1.21			
	A_6				40.20	40.10	39.40	40.09	40.26	1.29	1.20		51.5	110.1
	A_7	αα	B*BB*E	t					40.00		1.28, 1.33			
	A_8								39.85		1.18, 1.25			
	A_9				39.61, 39.56	39.45	39.00, 38.70	39.80	39.74	1.18, 1.24	1.21			
	A_{10}	CH	EE*B*EE	d				39.76	39.71	1.29	1.28	2.8		
	A_{11}	αα	E*BB*E	t	39.28, 38.98	38.80	38.10	39.21	39.17	1.20	1.20	0.7		
B	B_1	CH	EB*B*EE	d	37.24	37.20	36.40	37.45	37.39	1.38	1.39	2.1	7.5	66.9
	B_2	CH	EB*B*EB	d					37.31		1.38			
C	C_1	CH	BB*B*BB	d				35.23	35.19	1.47	1.48			
	C_2	CH	BB*B*BE	d					35.09		1.47			
	C_3	αγ	BB*E*BB	t	34.98, 34.81	34.80, 34.70−34.50	34.00		35.01		1.32			
	C_4	CH	EB*B*BE	d					35.01		1.48		102.2	188.6
	C_5	αγ	BB*E*BE	t					34.94		1.31			
	C_6	αγ	EB*E*BE	t	34.49	34.40	33.80	34.62	34.59	1.30	1.30	1.5		
	C_7	αδ$^+$	B*BE*E	t	34.33	34.20	33.60	34.46	34.46	1.32	1.31	1.5		
	C_8	αδ$^+$	E*BE*E	t	34.01	33.85	33.40	34.14	34.09	1.30	1.30	1.8		
D	D_1	γγ	B*EE*B	t	30.92	30.90	30.70	30.93	30.91	1.34	1.34	2.0	12.9	27.8
	D_2	γδ$^+$	B*EE*E	t	30.47	30.40	30.20	30.46	30.41	1.34	1.33	2.3	81.1	60.2
	D_3	δ$^+$δ$^+$	$(EEE)_n$	t	29.98	29.90	29.80	29.98	29.90	1.34	1.32	2.6	546.4	125.5
E	E_1	2B	EB*B*BE	t	27.70	27.6, 27.35	27.20	27.45	27.43	1.34	1.37		93.5	196.9
	E_2	βδ$^+$	E*BE*E	t	27.27	27.20	26.80	27.33	27.28	1.34	1.33	2.1		
	E_3	βδ$^+$	B*BE*E	t	27.10−26.80	27.00	26.60	27.17	27.14	1.35	1.35	1.7		
	E_4	2B	EB*B*EB	t					27.07		1.35			
	E_5	2B	EB*B*EE	t		26.80	26.30	27.12	27.01	1.35	1.35	1.5		
	E_6	2B	EE*B*EB	t					26.97		1.34			
	E_7	2B	EE*B*EE	t	26.68	26.50	26.10	26.79	26.71	1.34	1.33	2.2	47.3	50.9
F	F_1	ββ	EB*E*BE	t	24.54	24.40	23.90	24.68	24.63	1.36	1.36	1.6	7.6	29.6
	F_2	ββ	BB*E*BE	t	24.39	24.25	23.70		24.48		1.36			
	F_3	ββ	BB*E*BB	t	24.24	24.15			24.44		1.34			
G	G_1	1B	E*B*E	q	11.18	11.20	10.90	11.17	11.07	0.90	0.89	6.8	44.5	51.7
	G_2	1B	EE*B*EB	q					10.95		0.90			
	G_3	1B	EB*B*EE	q	11.00	11.00	10.70	11.02	10.89	0.91	0.90	7.1	5.5	64.2
	G_4	1B	EB*B*EB	q					10.82		0.90			
	G_5	1B	BB*B*BB	q					10.66		0.91			
	G_6	1B	BB*B*BE	q					10.60		0.90			
	G_7	1B	EB*B*BE	q	10.81	10.80	10.60		10.51		0.91			27.5

[a] DEPT and HSQC experiment results s, d, t and q are quaternary, methine, methylene, and methyl carbon resonances. [b] Relative to internal hexamethyldisiloxane (HMDS), estimated error 0.005 ppm based; digital resoution is 0.08 Hz/point (0.0004 ppm/point), with an average line width of 1 Hz. [c] Relative to internal hexamethyldisiloxane (HMDS), estimated error 0.005 ppm based. [d] Relative error better than 10%

in high-resolution 1D ^{13}C NMR spectra. A significant advantage of gHSQC over the gHMQC experiment reported in earlier studies[5] is the ability to use it for spectral editing to distinguish between methyl/methine resonances (positive cross-peaks) and methylene resonances (negative cross-peaks) in the spectra. This procedure helps to eliminate the need for DEPT analysis to determine the multiplicity of various resonances. Since the gHSQC experiment involves detection of ^1H (and indirect detection through ^1H of ^{13}C characteristics), it is possible to detect signals from low occurrence structures whose resonances are too weak to detected in the DEPT experiment which involves direct observation of ^{13}C. However, the drawback of the HSQC method is that, in cases where methyl or methine resonances overlap with methylene resonances, a phase distortion is produced in the spectrum that could hamper the recognition of both signals. Fortunately, in the present analyses, there are no such overlaps. Furthermore, improved resolution in gHSQC spectra compared to that in the gHMQC spectra provides clear distinction among various CH_n resonances which are not completely resolved in the 1D ^{13}C NMR spectrum. Parts c−e of Figure 2 show gHMBC spectra of copolymers A and B obtained using two different τ_{mb} values ($\tau_{mb} = 0.05$ and 0.1). Two different τ_{mb} values are used to collect two different spectra under conditions optimal for detection of cross-peaks from two- and three-bond $^1H-^{13}C$ couplings, which usually range from 2 to 12 Hz. One-bond C−H connectivity can be confirmed using the data in Figure 2, parts a and b. Most of the cross-peaks in Figure 2a result from structures associated with isolated ethyl branches of B-centered triads containing a single B unit. In Figure 2b, some additional cross-peaks are seen from structures with two or more contiguous B units. The methyl and methine resonances can be clearly distinguished from methylene resonances as the former two show inverted cross-peaks relative to the cross-peaks of the latter in gHSQC spectra. In the present case, all the methylene resonances appear as negative cross-peaks while both methyl and methine resonances appear as positive cross-peaks. The cross-peaks corresponding to methyl and methine resonances in Figure 1, parts a and b, are labeled as CH_3 (1B) and CH, respectively, and completely agree with the results from the DEPT experiment.

Figure 3 shows gHSQC and gHMBC correlations originating from the methyl groups of EBE and BBE triad sequences in copolymer A. The structures of these triads are shown above the 2D correlation plots. In these structures, the solid lines represent bonds present in the original monomers and the dashed lines represent the bonds formed between the two comonomer units during polymerization. Two one-bond methyl correlations (labeled with lower case letters) are seen in the gHSQC spectrum (Figure 3a) one from EBE sequences ($1B_{EBE}$, cross-peak a) at $\delta_C = 11.17$ ppm and $\delta_H = 0.90$ ppm and one from BBE sequences ($1B_{BBE}$, cross-peak b) at $\delta_C = 11.02$ ppm and $\delta_H = 0.91$ ppm. Both of these cross-peaks display three equally spaced contours in the proton dimension ($J = 7$ Hz) from homonuclear J coupling to adjacent protons. Throughout this manuscript, the convention is to label HMBC cross-peaks with a lower-case letter corresponding to the label of the HSQC cross-peak at the same ^1H chemical shift. Since there are many carbons that can be two or three bonds away from this proton, the labels of the resulting HMBC

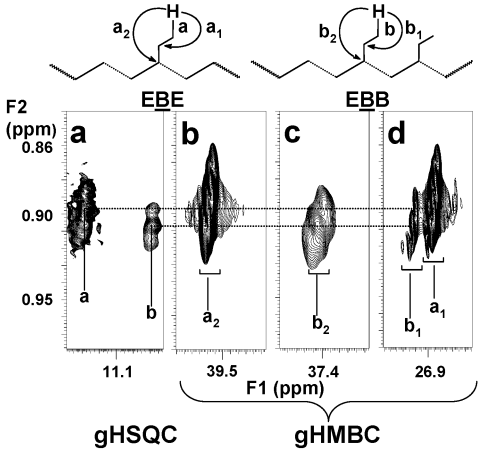

Figure 3. Expansions from the gHSQC and gHMBC spectra of copolymer A in the proton chemical shift region between 0.84 and 0.98 ppm: (a) gHSQC spectrum segment in the carbon chemical shift region between 10.9 and 11.2 ppm; (b−d) gHMBC spectrum segments in the carbon chemical shift regions between 38 and 40.0, 37.0 and 37.6, and 26.0 and 27.4 ppm, respectively.

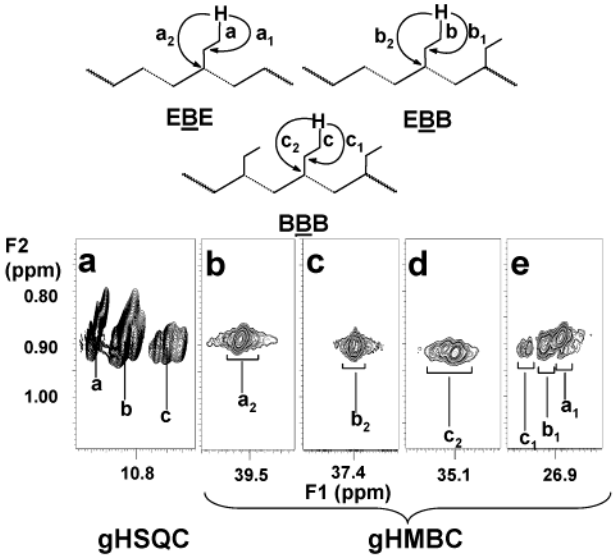

Figure 4. Expansions from the gHSQC and gHMBC spectra of copolymer B in the proton chemical shift region between 0.7 and 1.1 ppm: (a) methyl region of gHSQC spectrum segment in the carbon chemical shift region between 10.4 and 11.2 ppm; (b−e) gHMBC spectrum segments in the carbon chemical shift regions between 39 and 40.1, 36.0 and 38.8, 34.5 and 35.5, and 26.0 and 27.6 ppm, respectively.

cross-peaks are distinguished by numerical subscripts. The $1B_{EBE}$ proton has two and three bond H−C correlations to carbon $2B_{EBE}$ (cross-peak a_1, Figure 3d) at $\delta_C = 26.79$ ppm and to carbon CH_{EBE} (cross-peak a_2, Figure 3b) at $\delta_C = 39.76$ ppm in gHMBC spectrum. Similarly the $1B_{BBE}$ methyl protons have two and three bond correlations to carbon $2B_{BBE}$ (cross-peak b_1, Figure 3d) at $\delta_C = 27.12$ ppm and to carbon CH_{BBE} (cross-peak b_2, Figure 3c) at $\delta_C = 37.45$ ppm. These correlations help with unambiguous assignments of various "B"-centered triads. As the concentration of 1-butene in copolymer A is only 12%, the probability of $1B_{BBB}$ triads is low, and cross-peaks from these structures are not expected and are not evident in these spectra.

Figure 4 shows the H−C correlations of B-centered triads from copolymer B, originating from the three sets

of methyl gHSQC correlations. Even though only a single broad methyl resonance is observed in the ^{1}H spectrum the combined dispersion in two frequency dimensions is sufficient to resolve a considerable degree of fine structure in both the ^{1}H and ^{13}C dimensions. Three groups of one-bond methyl H−C correlations are seen in the gHSQC spectrum (Figure 4a): EBE sequences ($1B_{EBE}$, cross-peak cluster a), BBE sequences ($1B_{BBE}$, cross-peak cluster b), and BBB sequences ($1B_{BBB}$, cross-peak cluster c). The relative intensities of the 1D ^{13}C resonances in the spectra of the two copolymers (Figure 1) support these assignments. Parts b−e of Figure 4 contain regions from the gHMBC spectrum showing the two- and three-bond ^{1}H−^{13}C correlations to the methyl protons of "B"-centered triads. The $1B_{EBE}$ methyl proton resonance has two- and three-bond H−C correlations to carbon $2B_{EBE}$ (cross-peak a_1, Figure 4e) at $\delta_C = 26.71$ ppm and to carbon CH_{EBE} (cross-peak a_2, Figure 4b) at $\delta_C = 39.71$ ppm in gHMBC spectrum. The $1B_{BBE}$ methyl proton resonance has two- and three-bond H−C correlations to carbon $2B_{BBE}$ (cross-peak b_1, Figure 4e) at $\delta_C = 27.01$ ppm and to carbon CH_{BBE} (cross-peak b_2, Figure 4c) at $\delta_C = 37.39$ ppm. The $1B_{BBB}$ methyl proton resonance has two- and three-bond H−C correlations to carbon $2B_{BBB}$ (cross-peak c_1, Figure 4e) at $\delta_C = 27.43$ ppm, and to carbon CH_{BBB} (cross-peak c_2, Figure 4d) at $\delta_C = 35.15$ ppm. Furthermore, cross-peak c clearly shows three distinct correlations at $\delta_C = 10.51$, 10.60, and 10.66 ppm and corresponding $\delta_H = 0.91$, 0.90, and 0.91 ppm, matching well with the 1D ^{13}C NMR results. Similarly both c_1 and c_2 cross-peaks also show three cross-peaks in each cluster in the gHMBC spectrum (Figure 4, parts e and d, respectively). The separation of independent cross-peaks within the c_2 cross-peak cluster is more evident than that within the c_1 cross-peak cluster. Similar to observation in 1D ^{13}C NMR spectrum, gHSQC cross-peak b can be related to three distinct gHMBC cross-peaks at $\delta_C = 10.82$, 10.89, and 10.95 ppm and the corresponding methyl proton resonance $\delta_H = 0.90$ ppm. However, the cluster of cross-peaks b_1 and b_2 in the gHMBC spectra are partially overlapped so that only two of the cross-peaks in clusters b_1 and b_2 can be resolved. As stated above during the discussion of 1D ^{13}C NMR spectrum (Figure 1b), these multiple cross-peaks may originate from sensitivity of the chemical shifts to pentad comonomer distribution and/or stereosequence effects. However, it is necessary to closely examine the resonances related to the gHSQC cross-peaks of 2B methylene groups and CH groups at branch points to identify these structures, as CH_3 carbons are too far from the stereogenic centers of adjoining B units.

Figure 5a shows expansions of the regions from the gHSQC spectrum of copolymer B containing correlations from 2B and $\beta\delta$ methylene groups ($\delta_C = 26.5-27.6$ ppm). Parts b−e of Figure 5 show expansions of regions from the gHMBC spectrum of this polymer in the δ_H region of 1.0−1.7 ppm. There is extensive overlap of 2B and $\beta\delta$ resonances in Figure 5a. The initial assignments are based on previous work carried out by Cheng in 1991.[32] In total there are seven individual cross-peaks in the cluster corresponding to two types of $\beta\delta$ resonances and five types of 2B resonances as summarized in column 3 of Table 1. The cross-peak at $\delta_C = 26.71$ ppm and $\delta_H = 1.33$ ppm is assigned to methylene $2B_{EBE}$ (cross-peak, d) based on the single peak observed in the 1D ^{13}C spectrum of copolymer A having low 1-butene

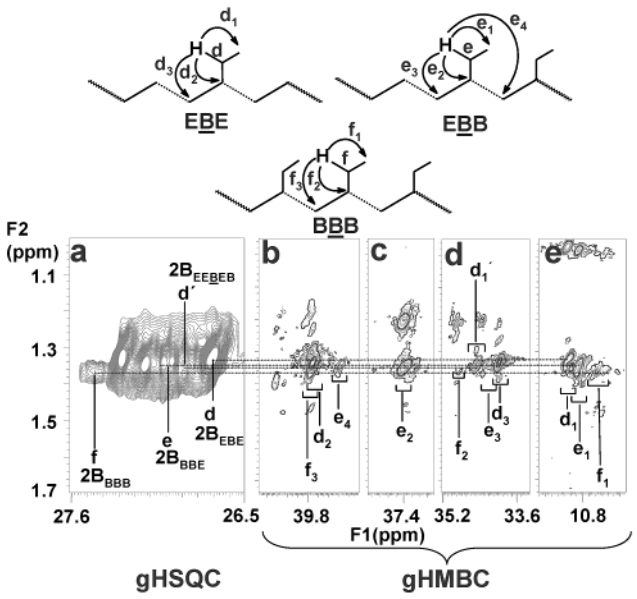

Figure 5. Expansions from the gHSQC and gHMBC spectra of copolymer B in the 2B proton chemical shift region between 1.0 and 1.7 ppm: (a) gHSQC spectrum segment in the carbon chemical shift region between 26.6 and 27.6 ppm; (b−e) gHMBC spectrum segments in the carbon chemical shift regions between 38.8 and 40.2. 37.0 and 37.8, 33.7 and 35.2, and 10.1 and 11.4 ppm, respectively.

content. Another cross-peak at $\delta_C = 26.88$ ppm and $\delta_H = 1.36$ ppm is resolved and may be assigned to $2B_{EEBEB}$ methylene group (cross-peak, d′). Two distinct cross-peaks at $\delta_C = 26.97$ and 27.01 ppm and $\delta_H = 1.34$ and 1.35 ppm, respectively, are due to $2B_{BBE}$ methylene groups (cross-peak, e). The observation of two distinct cross-peaks for $2B_{BBE}$ methylene groups matches with the results obtained for $1B_{BBE}$ cross-peaks. The cross-peak corresponding to $2B_{BBB}$ carbons (cross-peak, f) appears at $\delta_C = 27.43$ ppm and $\delta_H = 1.37$ ppm. As expected from the discussion above, there should be three contours corresponding to three $1B_{BBB}$ cross-peaks. Careful interpretation of this region indeed proves this point and it is possible to identify three cross-peaks at $\delta_C = 27.42$, 27.47, and 27.52 ppm (expanded plot shown in Supporting Information). These assignments are confirmed by the observation of long-range correlations in the gHMBC spectrum (Figure 5, parts b−e). Multiple bond H−C correlations are seen in the gHMBC spectrum between $2B_{EBE}$ protons and carbons $1B_{EBE}$ (cross-peaks, d_1) at $\delta_C = 11.07$ ppm, CH_{EBE} (cross-peak, d_2) at $\delta_C = 39.71$ ppm and $\alpha\delta^+_{EBEE}$ (cross-peak, d_3) at $\delta_C = 34.09$ ppm. Similarly, multiple bond H−C correlations are detected between $2B_{BBE}$ protons and carbons $1B_{BBE}$ (cross-peaks, e_1) at $\delta_C = 10.89$ ppm, CH_{BBE} (cross-peak, e_2) at $\delta_C = 37.39$ ppm, $\alpha\delta^+_{BBEE}$ (cross-peak, e_3) at $\delta_C = 34.46$ ppm and $\alpha\alpha_{EBBE}$ (cross-peak, e_4) at $\delta_C = 39.17$ ppm as shown in Figure 5, parts b−e. $2B_{BBB}$ protons show distinct cross-peaks in the gHMBC spectrum at $\delta_C = 10.60$ ppm ($1B_{BBB}$, f_1), $\delta_C = 35.10$ ppm (CH_{BBB}, f_2) and $\delta_C = 40.00$ ppm ($\alpha\alpha_{BBBE}$, f_3). Furthermore, a characteristic multiple-bond correlation of $2B_{EEBEB}$ protons with $\alpha\gamma_{EBEBE}$ carbons at $\delta_C = 34.59$ ppm (cross-peak, d_1') is observed in support of this assignment. These cross-peaks unequivocally prove the peak assignments in this congested region of the spectrum. Furthermore, three $2B_{BBB}$ cross-peaks in the gHSQC spectrum (Figure 5a) are observed, which correspond to multiple bond couplings between these

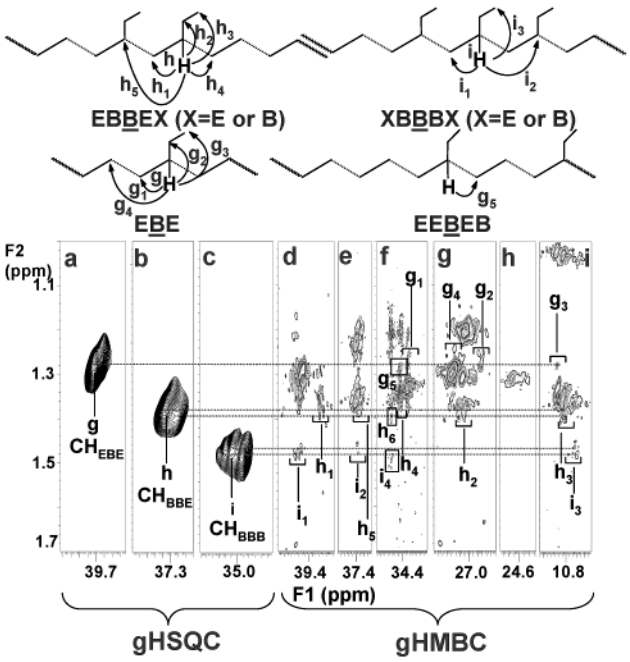

Figure 6. Expansions from the gHSQC and gHMBC spectra of copolymer B in the CH proton chemical shift region between 1.0 and 1.7 ppm: (a−c) gHSQC spectrum segments showing only CH cross-peaks in the carbon chemical shift regions between 39.5 and 39.9, 37.3 and 37.6, and 34.6 and 35.4 ppm; (d−i) gHMBC spectrum segments in the carbon chemical shift regions between 38.7 and 40.1, 37.0 and 37.8, 34.4 and 35.2, 26.4 and 27.6, 24.2 and 24.8, and 10.1 and 11.4 ppm, respectively.

three different protons and three different $1B_{BBB}$ carbons (cross-peak, f_1).

Parts a−c of Figure 6 contain three expansions from the gHSQC spectrum of copolymer B showing only methine resonances from three different types of "B"-centered triads. As mentioned above, methine and methylene carbons have opposite phases, thus it is possible to selectively plot CH or CH_2 cross-peaks by selecting either positive or negative contours. Broadly the methine region is divided into three clusters of cross-peaks from the three different methine groups of "B"-centered triads: CH_{EBE} ($\delta_C = 39.71$ ppm), CH_{BBE} ($\delta_C =$ 37.39 ppm), and CH_{BBB} ($\delta_C = 35.08$ ppm), which are displayed in parts a, b, and c of Figure 6, respectively. The complexity of these cross-peak patterns grows in parallel with the number of possible triad stereosequences for EBE, EBB and BBB triads. Parts d−i of Figure 6 show expansions from gHMBC spectra, spanning the complete ^{13}C chemical shift range of the aliphatic carbons of copolymer B, obtained with two different τ_{mb} values. However, unlike the gHSQC spectrum, the gHMBC correlations from other resonances including the main chain and branch sites are also observed, so these latter spectra are considerably more complex than the gHSQC spectrum. The lines connecting the spectra facilitate identification of the gHMBC correlations to the CH_{XBX} (X = E or B) proton chemical shifts of the cross-peaks identified in the gHSQC spectrum, and facilitate identification of these correlations in the complex gHMBC spectra. CH_{BBB} protons show cross-peaks from multiple bond H−C correlations to $\delta_C = 40.00$ ppm ($\alpha\alpha_{BBBE}$, i_1), $\delta_C = 37.39$ ppm (CH_{BBE}, i_2) and $\delta_C = 10.60$ ppm ($1B_{BBB}$, i_3). However, correlations from two-bond coupling between CH_{BBB} protons and $2B_{BBB}$ carbons were not detected. The CH_{BBE} protons show cross-peaks for multiple bond correlations at $\delta_H = 1.39$ ppm, with resonances of carbons which are two and three bonds away at $\delta_C = 39.17$ ppm ($\alpha\alpha_{EBBE}$, h_1), $\delta_C = 27.00$ ppm ($2B_{BBE}$, h_2), $\delta_C = 10.82$ ppm ($1B_{BBE}$, h_3), $\delta_C = 34.46$ ppm ($\alpha\delta^+_{BBEE}$, h_4), and $\delta_C = 37.39$ ppm (CH_{BBE}, h_5). Other methine resonances near $\delta_C = 39.79$ ppm, corresponding to CH_{EBE} groups, show similar multiple bond correlations in the gHMBC spectrum, at $\delta_C = 34.09$ ppm ($\alpha\delta^+_{EBEE}$, g_1), $\delta_C = 26.71$ ppm ($2B_{EBE}$, g_2), $\delta_C = 11.07$ ppm ($1B_{EBE}$, g_3), and $\delta_C = 27.28$ ppm ($\beta\delta^+_{EBEE}$, g_4).

Careful examination of Figure 6c shows the presence of three cross-peaks corresponding to three different CH_{BBB} carbons; these can be assigned to pentads CH_{BBBBB}, CH_{BBBBE}, and CH_{EBBBE}. The high field and dispersion of the signals into two frequency dimensions results in the resolution of resonances from pentads sequences, which were not observed in earlier one-dimensional NMR studies carried out at lower field. Distinct correlations are observed at $\delta_C = 35.05$ ppm (cross-peak i_4 (shown in square)) due to the multiple bond correlations of CH_{BBBBB} and CH_{BBBBE} carbons with $\delta_H = 1.50$ ppm (CH_{BBBBB} and CH_{BBBBE} protons). The CH resonance in Figure 6b also show two correlations assigned to CH_{EBBEE} and CH_{EBBEB} resonances in different tetrads. The assignment of CH_{EBBEB} resonances are be further confirmed by the distinct correlations of this protons with $\alpha\gamma_{BBEBB}$ carbons at $\delta_C = 35.01$ ppm (cross-peak h_6). Cross-peak g_5 is consistent with the presence of correlations between CH_{EEBEB} proton resonances at $\delta_H = 1.28$ ppm and $\alpha\gamma_{EBEBE}$ carbon resonances at $\delta_C =$ 34.59 ppm. However, the interpretation is tentative as other correlations, most importantly between CH_{EEBEB} protons and $\beta\beta_{EBEBE}$ carbons are not observed in the gHMBC spectra. These results are consistent with the cross-peak patterns observed in both 1B and 2B regions of the ($^1H-^{13}C$) gHSQC (Figures 4a and 5a) and ^{13}C NMR spectra (Figure 1b). Thus, it is evident that three distinct contours observed in Figure 4a (cross-peak, c) and Figure 5a (cross-peak, f) can be attributed to pentad comonomer sequences such as BB*B*BB, BB*B*BE, and EB*B*BE. The usual triplet pattern expected from these *n*-ad sequences is evident in 2D gHSQC spectrum (Figure 4a), and is clearly resolved in the expansion of the methyl region from the ^{13}C NMR spectrum (Supporting Information). In fact, careful examination of this region of the ^{13}C NMR spectrum indicates that additional fine structure from pentad stereosequence effects are partially resolved in the methyl BBB triplet resonances at 10.60 ppm. Two contours observed in Figure 6b, correspond with the 2B and 1B resonances represented as distinct cross-peaks in Figure 4a (cross-peak, b) and Figure 5a (cross-peak, e). These resonances may be assigned to two different pentad configurations such as EB*B*EE and EB*B*EB. This assignment is clear from the data presented in all the three figures corresponding to 1B, 2B, and CH resonances. The inability to clearly resolve separate contours from stereosequence effects might be due to lack of digital resolution in the gHSQC and gHMBC spectra.

A complete set of ^1H and ^{13}C resonance assignments, based on the interpretation of the 2D gHSQC and gHMBC NMR spectra of copolymers A and B, is presented in Table 1. The quantitative determination of comonomer content and monomer sequence distribution can be accurately determined based on these assignments.

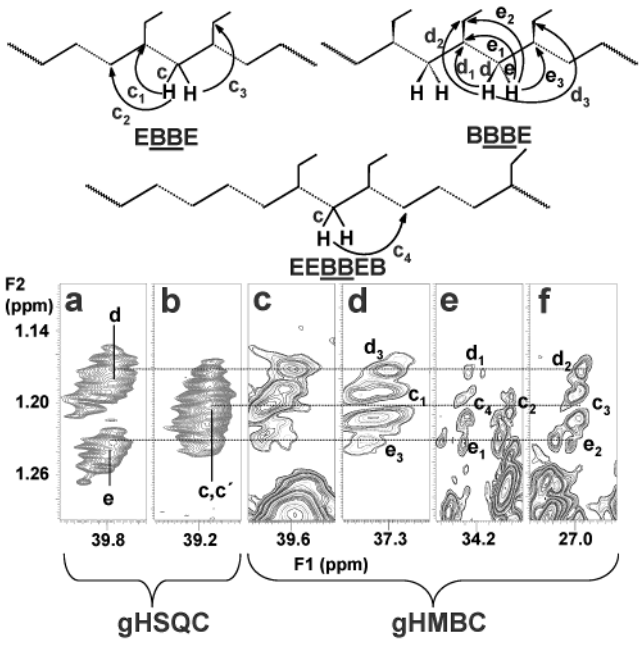

Figure 7. Expansions from the gHSQC and gHMBC spectra of copolymer A in the αα proton chemical shift region between 1.1 and 1.3 ppm: (a, b) gHSQC spectrum segments showing only CH_2 cross-peaks in the carbon chemical shift regions between 39.75 and 39.86 and 39.15 and 39.30 ppm; (c−f) gHMBC spectrum segments in the carbon chemical shift regions between 39.5 and 39.8, 37.24 and 37.42, 33.8 and 34.6, and 26.7 and 27.4 ppm, respectively.

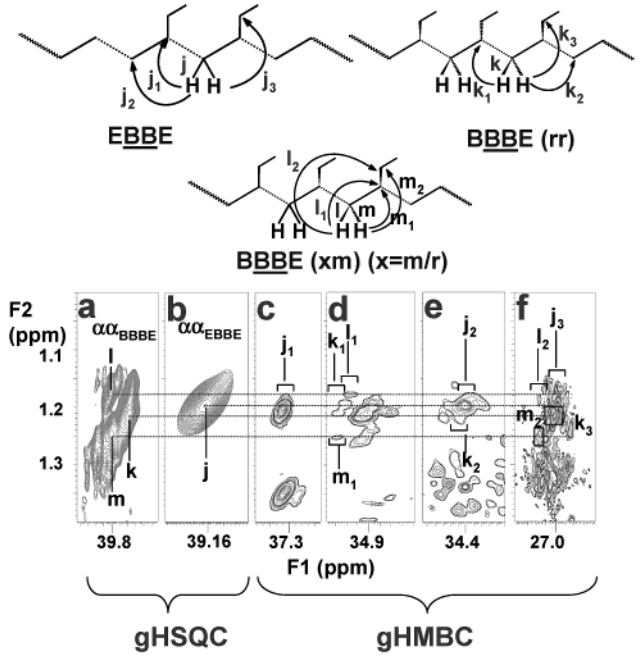

Figure 8. Expansions from the gHSQC and gHMBC spectra of copolymer B in the αα proton chemical shift region between 0.9 and 1.4 ppm: (a, b) gHSQC spectrum segments showing only CH_2 cross-peaks in the carbon chemical shift regions between 39.5 and 40.0 and 39.05 and 39.40 ppm; (c−f) gHMBC spectrum segments in the carbon chemical shift regions between 37.1 and 37.6, 34.75 and 35.15, 34.2 and 34.7, and 26.6 and 27.4 ppm, respectively.

Stereosequence Information from 2D gHSQC and gHMBC of Poly(ethylene-*co*-1-butene). In determining a polymer's microstructure, tacticity and degree of stereoregularity are two key features of copolymers which must be ascertained. In the case of ethylene-α-olefin copolymerization, observation of tacticity information in the ^{13}C NMR spectra has been widely cited; however, in the case of ethyelne-*co*-1-butene copolymers definitive proof of resonances assignments has not been reported. Randall showed the presence of both meso (*m*) and racemic (*r*) isolated BB diads from the resonances of $\alpha\alpha_{EBBE}$ groups.[31] However, stereosequence information regarding *n*-ads with runs larger than two units (e.g., B*BB*E and B*BB*B tetrads) is not available from the αα-CH_2 resonance patterns in this region of 1D ^{13}C NMR spectrum. Thus, it would be extremely useful if the data provided this type of tacticity information. The two αα-CH_2 protons are nonequivalent in the case of meso diads and approximately equivalent in the case of racemic diads. Thus, 2D $^1H-^{13}C$ correlation NMR technique such as HSQC should be used to obtain such information. The αα-carbon resonances of meso diads will be correlated with two αα-proton resonances corresponding to two directly bonded nonequivalent protons, and the αα-carbon resonances of racemic diads will be correlated with a single proton resonance from the chemically equivalent racemic αα-protons. In the case of ethylene-1-butene copolymers, αα-methylene correlations show different cross-peak patterns depending on the stereosequence.

Parts a and b of Figure 7 show expansions of the αα-methylene regions from the gHSQC spectrum of copolymer A. From these figures, it is clearly observed that there are two sets of cross-peak patterns at $\delta_C = 39.80$ ppm, relating this carbon resonance to protons at $\delta_H = 1.18$ (cross-peak, d) and 1.24 ppm (cross-peak, e). This clearly indicates the presence of B*BB*E tetrads containing a central meso BB diad. The absence of additional resonances at slightly different carbon chemical shifts (as are observed for copolymer B, cross-peak k in Figure 8a, vide infra) shows that *mm* triads are the only species present at detectable levels in this region of the gHSQC spectrum of copolymer A.[53] However, separate clusters of cross-peaks are not observed at $\delta_C = 39.21$ ppm and the corresponding proton shift of $\delta_H = 1.20$ ppm. This is not because the E*BB*E tetrad sequences of this copolymer all racemic in nature. Rather, it is due to the fact that the chemical shift difference between the geminal methylene protons c and c′ are smaller in meso E*BB*E tetrads than the chemical shift difference of the corresponding protons in the central meso diads of B*BB*E tetrads. The latter explanation is more reasonable as the c/c′ cross-peak pattern in Figure 7b is too broad to be from proton−proton homonuclear coupling alone (A representative cross-peak pattern from racemic E*BB*E tetrads is seen in the spectrum of copolymer B, cross-peak j, Figure 8b, vide infra). Parts c−f of Figure 7 show expanded regions from the gHMBC spectrum of copolymer A in the proton chemical shift range of 1.1−1.3 ppm. Multiple bond correlations between the resonances of $\alpha\alpha_{EBBE}$ methylene protons and the resonances of various carbons are observed at $\delta_C = 37.45$ ppm (CH_{EBBEE}, c_1), $\delta_C = 34.46$ ppm ($\alpha\delta^+_{BBEE}$, c_2), and $\delta_C = 27.12$ ($2B_{BBE}$, c_3). The line drawn parallel to the center of the $\alpha\alpha_{EBBE}$ cross-peak passes through the middle of two cross-peaks equally spaced from the center in each expansion of gHMBC spectrum. This indicates that although there is poor resolution in ^1H dimension of the gHSQC spectrum, in gHMBC spectrum there is enough resolution to show two different cross-peaks at each carbon shift, consistent with the assignment of these resonances to meso BB diads in E*BB*E tetrads. This

observation proves that the chemical shift difference between two nonequivalent αα-CH_2 protons of the meso BB diads in centered in E*BB*E tetrads is small compared to the corresponding shift difference of meso BB diad stereosequences centered in B*BB*E tetrad. This suggests that copolymer A contains essentially all meso diads in E*BB*E and B*BB*E tetrads. Three long-range correlations for each cross-peak in Figure 7a are clearly labeled in the gHMBC spectra and are consistent with this assignment.

Parts a and b of Figure 8 show expansions of the αα-methylene regions from the gHSQC spectrum of copolymer B. In contrast to the results from copolymer A, these regions are more complex and there is considerable overlap of resonances. Figure 8b shows one broad cross-peak from the αα carbons in E*BB*E tetrads at δ_C = 39.17 ppm. Parts c−f of Figure 8 show expanded regions from the gHMBC spectrum of copolymer B in the proton chemical shift range (δ_H) of 1.0−1.4 ppm. Multiple bond correlations between the resonance of $\alpha\alpha_{EBBE}$ protons and various carbon resonances are observed at δ_C = 37.39 ppm (CH_{EBBEE}, j_1), δ_C = 34.46 ppm ($\alpha\delta^+_{BBEE}$, j_2), and δ_C = 27.01 ($2B_{BBE}$, j_3). Unlike the gHSQC spectrum of copolymer A (Figure 7), in the spectrum of this sample, there is only one single contour which can be seen both in gHSQC and gHMBC spectrum. This result indicates that essentially all the $\alpha\alpha_{EBBE}$ units are racemic in nature corresponding to syndiotactic nature of the triad comonomer sequences. The width of cross-peak j in Figure 8b is ca. 75 Hz in the F2 (^{1}H chemical shift) dimension, whereas the width of cross-peaks c/c′ in Figure 7b (attributed to *meso* diads, vide supra) is almost twice as large. This is consistent with j and c/c′ cross-peaks arising from *racemic* and *meso* diads, respectively. The cross-peak patterns from copolymer B in Figure 8a are more complex than those seen in the corresponding regions of the spectra from copolymer A (Figure 7a). It is possible to detect at least three well-resolved sets of cross-peaks. The most intense cross-peak, k, at δ_C = 39.74 ppm and δ_H = 1.21 ppm, shows single cross-peak and can be assigned to $\alpha\alpha_{BBBE}$ tetrads having a racemic central diad configuration. Furthermore, there are two equally spaced cross-peaks at δ_C = 39.85 ppm corresponding to δ_H = 1.18 and 1.25 ppm. This shows that B*BB*E tetrads are not completely racemic but a mixture of both meso and racemic diad stereosequences. Two multiple bond correlations are observed for each cross-peak, labeled l_1 and m_1 at δ_C = 35.01 ppm (CH_{EBBBE}) and l_2 and m_2 at δ_C = 37.43 ppm ($2B_{BBB}$). Although there is a small contribution of resonances from $\alpha\alpha_{BBBE}$ (*rm*) sequences to the signals in this region, this contribution is relatively low compared to the contribution from signals of pure racemic diads (*rr*) in B*BB*E tetrad sequences.

Figure 9 shows an expansion from the gHSQC spectrum of copolymer B between δ_C = 40.2−40.6 ppm displaying the numerous cross-peaks observed for αα methylene groups of B*BB*B tetrad stereosequence. Expansion of 1D ^{13}C NMR spectrum of copolymer B between δ_C = 40.2−40.6 ppm is displayed on the top of the gHSQC spectrum. In total, six different sets of resonances at six different δ_C values can be isolated; the corresponding chemical shifts are shown as A_1 to A_6 in Table 1. These six resonances can be correlated to six possible BBBB tetrad stereosequences: *mrm*, *mrr*/*rrm*, *rrr*, *rmr*, *mmr*/*rmm*, and *mmm*. There is only slight difference between the BBBB tetrad chemical shifts for

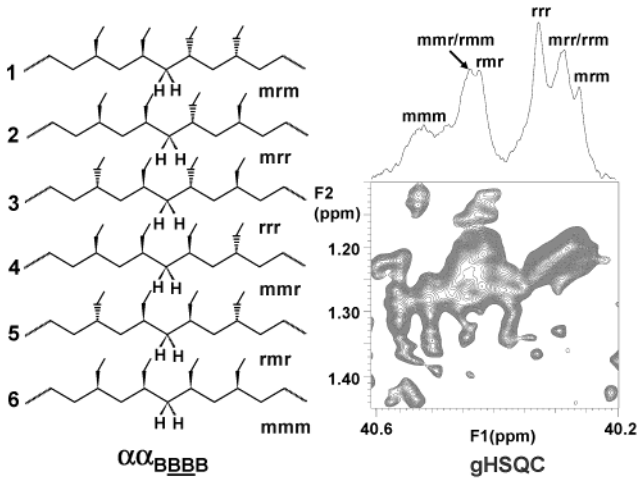

Figure 9. Expansions from the gHSQC spectrum of copolymer B in the $\alpha\alpha_{BBBB}$ proton chemical shift region between 1.10 and 1.45 ppm showing cross-peaks from tacticity effect.

the αα-methylene groups in each of these stereosequences due to the slight chemical shift perturbation. Thus, considering the neighboring stereochemistry, it is possible to suggest shift patterns along carbon chemical shift dimension for different isomers as shown in Figure 9. In the 1D ^{13}C spectrum, the region δ_C = 40.2−40.4 ppm contains three partially resolved resonances corresponding to three *r*-centered triads: *mrm*, *mrr*/*rrm*, and *rrr*. Similarly, the gHSQC spectrum shows three overlapping patterns consistent with these three structures. The resonances due to *m*-centered triads *mmm*, *mmr*/*rmm*, and *rmr* appear downfield at δ_C = 40.4−40.6 ppm. In this region of the 1D ^{13}C spectrum, three groups of resonances can be distinguished that correspond to clusters of cross-peaks in the gHSQC spectrum. As expected these resonances show multiple cross-peaks in the proton dimension, and at least four cross-peaks can be identified at each carbon chemical shift position. The spectral features in Figure 9 indicate that most of these higher B stereosequence are from a mixture of meso and racemic diads. As these resonances are less intense compared to other resonances, corresponding multiple bond correlation in the gHMBC spectrum are not detected. The possibility of overlapping resonances from pentad stereosequence cannot be ruled out and the complex cross-peak patterns further substantiate this interpretation. The spectral features are consistent with a predominance of signals from r diad sequences in copolymer B, although long B sequences are essentially mixture of both m and r conformations.

Quantitative Analysis of Poly(ethylene-*co*-1-butene). For quantitative analysis, 1D ^{13}C NMR experiment was carried out with a relaxation delay of almost five times the longest observed T_1 to ensure uniform recovery of the equilibrium magnetization for all the carbons of interest.[54] The relaxation delay used depends on the degree of accuracy needed in the final analysis. Nuclear Overhauser enhancements are full for aliphatic carbon resonances. This is consistent with rapid motion compared to the spectrometer frequency (extreme narrowing condition satisfied), as is expected for essentially linear polymers at the high temperatures used to acquire the spectra in this work. Values for the carbon T_1's of poly(ethylene-1-butene) with ca. 12% 1-butene contents are listed in columns 13 of Table 1. These range from 0.7 s for αα methylene carbons to 7.1 s for the methyl carbons (N×T_1 consistent with relax-

Table 2. Estimation of Polymer Compositions

			copolymer triad compositions (%)					
	formulas for triad compositional analysis		copolymer A (E/B = 88:12)			copolymer B (E/B = 59:41)		
structure	Randall[a]	this work	Randall[a]	this work	Bernoullian[b]	Randall[a]	this work	Bernoullian[c]
[EBE] =	k(C−A−$^1/_2$B)	kG$_1$	10.40	9.96	9.40	12.56	14.38	14.27
		kE$_7$		10.61			14.16	
		average		10.28			14.27	
[EBB+BBE] =	kB	kB	1.66	1.68	2.61	18.68	18.61	19.84
		average		1.68			18.61	
[BBB] =	k(2A−C)	k(2A−C)	0.18	0.19	0.18	8.83	8.80	6.89
		k(G$_5$+G$_6$+G$_7$)					7.64	
		average		0.19			8.22	
[BEB] =	kF	k(F$_1$+F$_2$+F$_3$)	1.68	1.70	1.31	8.27	8.24	9.92
		average		1.70			8.24	
[BEE+EEB] =	k(E−G)	k(E−G)	20.14	20.37	18.81	29.14	29.03	28.54
		average		20.37			29.03	
[EEE] =	$^1/_2k$(D−$^1/_2$E+$^1/_2$G))	D$_3$/2+D$_2$/4	65.93	65.78		22.52	21.63	20.54
		average		65.78	67.68		21.63	
% [E] =	[EEE+EEB/BEE+BEB]	[EEE+EEB/BEE+BEB]	87.76	87.85		59.92	58.90	
% [B] =	[BBB+BBE/EBB+EBE]	[BBB+BBE/EBB+EBE]	12.24	12.15		40.08	41.10	

[a] Reference 31. [b] Based on 12.2% A. [c] Based on 41.0% B.

ation in the extreme narrowing regions). As expected, the carbons in the ethyl branches show large T_1's compared to the carbons in the main chain due to their greater mobility.

A complete summary of the NMR resonance assignments and region integrals are contained in Table 1. The first column of Table 1 contains region labels first designated by Hsieh and Randall based on the limited number of resolvable peaks in their lower field spectra.[30,31] The greater dispersion at higher field permits these regions to be further divided into subregions as shown in the second column of Table 1. Assignments for each of the regions are presented in columns 3 (carbon type) and 4 (comonomer sequence). Some assignments from the literature are shown in columns 6−8. Columns 9 and 10 summarize the ^{13}C chemical shift data, and columns 11 and 12 summarize ^{1}H chemical shift data of two copolymers based on analysis of the 2D NMR spectra presented here.

Table 2 shows the result from compositional analysis of copolymers A and B, based on the integral data presented in Table 1. The second column of Table 2 contains some empirical formulas to calculate monomer sequence distribution using the relationships given by Hsieh and Randall.[30,31] Because unique resonances are not resolved for each structure unit, it was necessary to use a collective assignment method, where linear combinations of the peak areas in region A−G of the 1D spectrum from groups of resolvable peaks are related to the concentrations of combinations of structure units such as triads and tetrads. A set of linear equations was obtained, relating the integral values in each region to the concentrations of *n*-ads contributing to the peaks in that region. Algebraic manipulation of terms yielded expressions relating triad concentrations to linear combinations of peak region integrals. These relationships are summarized in column 2 of Table 2. In all case, k is a scaling constant that relates the number of structure fragments to the absolute NMR signal intensities. Because relative concentrations of species are calculated, it is not necessary to know the value of k.

Because the high field NMR spectrometer provides high resolution and dispersion in the ^{13}C spectra, it is possible, and preferable, to directly relate concentrations of structure fragments to individual peak areas. In this way, more accurate compositions can be determined. Some new formulas based on these newly resolved peak regions are given in the third column of Table 2. In many cases, there is more than one resolved integral region that can serve as a measure for the amount of a triad. In these instances, the results from multiple determinations can in some instances be averaged to further reduce the error associated with the composition calculations. Results from the compositional analysis of copolymer A and B are summarized in columns 5 and 8 of Table 2.

Conclusions

High-field 188.6 MHz ^{13}C NMR and modern 2D NMR methods such as gHSQC and gHMBC techniques provided high quality spectra for unambiguous resonance assignments of microstructures present in poly(ethylene-*co*-1-butene). These results confirm most of the resonance assignments reported in the literature, and resolve several disagreements of ^{13}C chemical shift assignments. Better resolution at 750 MHz is enough to isolate many unique resonances from higher *n*-ad structures. High-resolution phase-sensitive gHSQC and gHMBC can be used to distinguish resonances for each structure and offer unambiguous proof to assign resonances and to study the tacticities of copolymers synthesized with different metallocene catalyst systems. It is clearly demonstrated that two polymers presumably prepared in different ways, and having different comonomer content (concentration of 1-butene), exhibit different tacticities; i.e., copolymer A contains essentially all meso B sequences while copolymer B is a mixture of both meso and racemic B sequences with predominant racemic configurations. Better dispersion in the 188.6 MHz ^{13}C 1D spectra permit the separate measurement of more individual integral regions. Under these circumstances, it is possible to relate most triads to distinct regions of the spectrum. In many cases, several independent integral measurements can be made for each triad from different regions of the spectrum; these can be averaged to give more reliable results.

Acknowledgment. We wish to acknowledge the National Science Foundation (DMR-9617477 and DMR-0073346) for support of this research and the Kresge Foundation and donors to the Kresge Challenge program at the University of Akron for funds used to

purchase the 750 MHz NMR instrument used for this work. Thanks are due to Simon Stakleff and Joe Massey for their support in maintaining the NMR facilities used in this work.

Supporting Information Available: Figures showing ^{13}C DEPT NMR subspectra of CH_n ($n = 1-3$) distributions, the ^{13}C NMR spectrum of the expanded methyl region, comparison of the gHMQC spectrum, the gHSQC spectrum, and the gHSQC NMR spectrum after linear prediction showing the resolution enhancement, individual spectra showing positive and negative cross-peaks from the gHSQC spectrum (copolymer B), and the expanded $2B_{BBB}$ region of the gHSQC spectrum. This material is available free of charge via the Internet at http://pubs.acs.org.

References and Notes

(1) Krentsel, B. A.; Kissin, Y. V.; Kleiner, V. J.; Stotskaya, L. L. *Polymers and Copolymers of Higher* α*-olefins*; Hanser/Gardner Publication: New York, 1997.
(2) Sinn, H.; Kaminsky, W. *Adv. Organomet. Chem.* **1980**, *18*, 99.
(3) Mcknight, A. L.; Waymouth, R. M. *Chem. Rev.* **1998**, *98*, 2587.
(4) Olabisi, O.; Atiqullah, M.; Kaminsky, W. *Rev. Macromol. Chem. Phys.* **1997**, *C37(3)*, 519.
(5) Liu, W.; Rinaldi, P. L.; McIntosh, L. H.; Quirk, R. P. *Macromolecules* **2001**, *34*, 4757.
(6) Kaminsky, W.; Arndt, M. *Adv. Polym. Sci.* **1997**, *127*, 143.
(7) Forguson, R. C. Trans. N. Y. *Acad. Sci.* **1967**, *29*, 495.
(8) Heatley, F.; Zambelli, A. *Macromolecules* **1969**, *6*, 618.
(9) Tonelli, A. E.; Schilling, F. C. *Acc. Chem. Res.* **1981**, *14*, 233.
(10) Schilling, F. C.; Bovey, F. A.; Bruch, M. D.; Kozlowski, S. A. *Macromolecules* **1985**, *18*, 1418.
(11) Bovey, F. A.; Mirau, P. A. *NMR of Polymer*; Academic Press: San Diego, CA, 1996.
(12) Bruch, M. D.; Bovey, F. A.; Cais, R.E. *Macromolecules* **1984**, *17*, 2547.
(13) Cheng, H. N.; Lee, G. H. *Trends Anal. Chem.* **1990**, *9*, 285.
(14) Cheng, H. N.; Lee, G. H. *Polym. Bull. (Berlin)***1985**, *13*, 549.
(15) Cheng, H. N.; Lee, G. H. *J. Polym. Sci., Part B: Polym. Phys.* **1987**, *25*, 2355.
(16) Benn, R.; Gunther, H. *Angew. Chem., Int. Ed. Engl.* **1983**, *22*, 350.
(17) Aue, W. P.; Bartholdi, E.; Ernst, R. R. *J. Chem. Phys.* **1976**, *64*, 2229.
(18) Li, L.; Rinaldi, P. L. *Macromolecules* **1997**, *30*, 520.
(19) Tokles, M.; Keifer, P. A.; Rinaldi, P. L. *Macromolecules* **1995**, *28*, 3944.
(20) Chai, M.; Saito, T.; Pi, Z.; Tessier, C.; Rinaldi, P. L. *Macromolecules* **1997**, *30*, 1240.
(21) Li, L.; Rinaldi, P. L. *Macromolecules* **1996**, *29*, 4808.
(22) McCord, E. F.; Shaw, W. H., Jr.; Hutchinson, R. A. *Macromolecules* **1997**, *30*, 246.
(23) Liu, W.; Ray, D. G., III; Rinaldi, P. L.; Zens, T. *J. Magn. Reson.* **1999**, *140*, 482.
(24) Liu, W.; Ray, D. G., III; Rinaldi, P. L. *Macromolecules* **1999**, *32*, 3817.
(25) Bax, A.; Summers, M. F. *J. Am. Chem. Soc.* **1986**, *108*, 2093.
(26) Hurd, R. E. *J. Magn. Reson.* **1990**, *87* (2), 422.
(27) Ray, G. J.; Spanswick, J.; Knox, J. R.; Serres, C. *Macromolecules* **1981**, *14*, 1323.
(28) Dechter, J. J.; Mandelkern, L. *J. Polym. Sci., Part B: Polym. Phys.* **1980**, *18*, 1955.
(29) (a) Florence, M.; Loustalot, G. *J. Polym. Sci., Polym. Chem. Ed.* **1983**, *21*, 2683. (b) Kimura, K.; Shigemura, T.; Yuasa, S. *J. Appl. Polym. Sci.* **1984**, *29*, 3161.
(30) Hsieh, E. T.; Randall, J. C. *Macromolecules* **1982**, *15*, 353.
(31) Randall, J. C. *J. Macromol. Sci.—Rev. Macromol. Chem. Phys.* **1989**, *C29* (2&3), 201.
(32) Cheng, H. N. *Macromolecules* **1991**, *24*, 4813.
(33) Cheng, H. N. *Polym. Bull. (Berlin)***1990**, *23*, 589.
(34) Rossi, A.; Zhang, J.; Odian, G. *Macromolecules* **1996**, *29*, 2331.
(35) Lee, D. H.; Jho, J. Y. *Polym. Bull. (Berlin)* **1997**, *38*, 665.
(36) Crist, B.; Howard, P. R. *Macromolecules* **1999**, *32*, 3057.
(37) Crist, B.; Claudio, E. S. *Macromolecules* **1999**, *32*, 8945.
(38) Vanden, E. S.; Mathot, V.; Koch, M. H. J.; Reynaers, H. *Polymer* **2000**, *41*, 3437.
(39) Striegel, A. M.; Krejsa, M. R. *J. Polym. Sci., Part B: Polym. Phys.* **2000**, *38(23)*, 3120.
(40) Pandey, G. C. *Process Control Qual.* **1995**, *7* (3−4), 173.
(41) Busico, V.; Cipullo, R.; Segre, A. L. *Macromol. Chem. Phys.* **2002**, *203*, 1403.
(42) Mueller, L. *J. Am. Chem. Soc.* **1979**, *101*, 4481.
(43) Bax, A.; Griffey, R. H.; Hawkins, B. L. *J. Am. Chem. Soc.* **1983**, *105*, 7188.
(44) Hurd, R. E.; John, B. K. *J. Magn. Reson.* **1991**, *91*, 648.
(45) Bax, A.; Subramanian, S. *J. Magn. Reson.* **1986**, *67*, 565.
(46) Pegg, D. T.; Doddrell, D. M.; Bendall, M. R. *J. Chem. Phys.* **1982**, *77*, 2745.
(47) Canich, J. A. M. (Exxon). PCT Int. Appl. WO 96/00244, 1996.
(48) Soga, K.; Uozumi, T. Nakamura, S.; Toneri, T.; Teranishi, T.; Sano, T.; Arai, T.; Shiono, T. *Macromol. Chem. Phys.* **1996**, *197*, 4237.
(49) McIntosh, L. H., III. Ph.D. Dissertation, University of Akron, December, 2000.
(50) States, D. J.; Haberkorn, R. A.; Ruben, D. J. *J. Magn. Reson.* **1982**, *48*, 286.
(51) Carman, C. J.; Wilkes, C. E. *Rubber Chem. Technol.* **1971**, *44*, 781.
(52) Parella, T. *Magn. Reson. Chem.* **1998**, *36*, 467.
(53) Note that the signal at 39.80 ppm in the 1D ^{13}C spectrum contains contributions from both $\alpha\alpha_{BBBE}$ (methylene) and CH_{EBE} (methine) carbons. However, the one-bond C−H correlations in the gHSQC spectrum, from these signals, are inverted with respect to one another. Since only negative contours are plotted in this figure, only CH_2 cross-peaks are observed.
(54) Farrar, T. C.; Becker, E. D. *Pulse and Fourier Transform NMR*; Academic Press: New York, 1969.

MA030056O